의학석사 학위논문

Malignant Potential Assessment of Intraductal Papillary Mucinous Neoplasms of the Pancreas: Comparison between Multidetector CT and MR Imaging with MR Cholangiopancreatography

췌장 IPMN의 악성도 평가
: Multi detector CT와 MR/MRCP의 비교

2015년 2월

서울대학교 대학원 임상의과학과

강 효 진

A thesis of the Master's Degree

췌장 IPMN의 악성도 평가

: Multidetector CT와 MR/MRCP의 비교

Malignant Potential Assessment of Intraductal Papillary Mucinous Neoplasms of the Pancreas: Comparison between Multidetector CT and MR Imaging with MR Cholangiopancreatography

February 2015

The Department of Clinical Medical Sciences,

Seoul National University

College of Medicine

Hyo-Jin Kang

Malignant Potential Assessment of Intraductal Papillary Mucinous Neoplasms of the Pancreas: Comparison between Multidetector CT and MR Imaging with MR Cholangiopancreatography

by

Hyo-Jin Kang

A thesis submitted to the Department of Clinical Medical Sciences in partial fulfillment of the requirements for the Master's Degree in Clinical Medical Sciences at Seoul National University College of Medicine

February 2015

Approved by Thesis Committee:

Professor _____Chairman

Professor _____Vice chairman

Professor _____

ABSTRACT

Introduction*:* To compare the diagnostic performances of multidetector computed tomography (MDCT) and magnetic resonance imaging (MRI) with MR cholangiopancreatography (MRCP) in predicting the malignant potential of pancreatic intraductal papillary neoplasms (IPMN) and to evaluate their inter-modality agreement.

Material and Methods: Institutional review board approval was obtained and the requirement for informed consent was waived for this retrospective study. In 129 patients with pathologically-proven pancreas IPMNs, three reviewers independently evaluated their preoperative MDCT and MRI with MRCP findings. Inter-modality agreement between MDCT and MRI with MRCP as well as interobserver agreement of each imaging modality in detecting high-risk stigmata and worrisome features were assessed. Diagnostic values of other signs of overt malignancy including the presence of “parenchymal mass” and “locoregional extension” were analyzed. Diagnostic performances and inter-modality consistency were assessed using receiver operating curve (ROC) analysis and weighted κ statistics.

Results: Overall predictability of MDCT and MRI with MRCP for the malignancy potential of pancreatic IPMNs was similar (AUC: 0.82 and 0.82, respectively) with good inter-modality agreement (κ=0.75) and moderate interobserver agreement (κ=0.47~0.59) when we set high-grade dysplasia as the cutoff for malignancy. When parenchymal masses and locoregional extensions were considered as overt malignant signs, invasive IPMN predictability was significantly increased (AUC: 0.87 for CT and 0.88 for MRI) with high sensitivity (94.3%) and equivocal specificity (69.1%).

Conclusion: Diagnostic performances in predicting the malignant potential of pancreatic IPMNs using MDCT and MRI with MRCP were similar while showing good inter-modality agreement, suggesting that interchangeable follow-up may be possible

---

Keywords: Pancreas IPMN, Malignant potential, Computed tomography (CT), Magnetic resonance imaging (MRI), MR cholangiopancreatography (MRCP)

Student number: 2013-22593

CONTENTS

LIST OF TABLES AND FIGURES

Appendix

LIST OF ABBREVIATIONS

ADC = apparent diffusion coefficient

AUC = area under the curve

DWI = diffusion-weighted imaging

EUS = endoscopic ultrasound

GRE = gradient echo

IPMNs = intraductal papillary mucinous neoplasms

MDCT = multi-detector row computed tomography

MPD = main pancreatic duct

MRI = magnetic resonance imaging

MRCP = magnetic resonance cholangiopancreatography

ROC = receiver operating characteristic

WHO = World Health Organization

INTRODUCTION

With the increasing use of multidetector computed tomography (MDCT) and magnetic resonance (MR) imaging for the evaluation of abdominal diseases, there has been a corresponding increase in incidentally detected pancreatic cystic lesions including intraductal papillary mucinous neoplasms (IPMNs) (1-3). IPMNs are defined as grossly visible intraductal epithelial neoplasms showing papillary proliferations and cyst formations (4, 5), and have histologically been shown to exhibit a wide spectrum of dysplastic changes from low and moderate grade dysplasia to high grade dysplasia (in situ carcinoma) to eventually, invasive carcinoma (6-8). Given that the detection of IPMNs in the early stage of carcinogenesis provides a unique opportunity to perform resection before they become invasive ductal carcinomas, evaluation of the malignant potential of pancreas IPMNs on cross sectional imaging modalities is crucial (4). However, considerable variability in interobserver agreements and radiologists' recommendations for pancreatic cystic lesions has been reported thus far (4, 9, 10). According to the International consensus guidelines 2012 for the management

of IPMNs and mucinous cystic neoplasms (MCNs) (11), two “high-risk stigmata” and six “worrisome features” on imaging studies such as CT or MR imaging were suggested to predict the malignant potential of IPMNs. As an example, ″high-risk stigmata” of an enhanced solid component and dilation of the main pancreatic duct (MPD) to a diameter greater than 10 mm has been strongly suggested to necessitate surgical resection. To the contrary, the presence of worrisome features such as cysts ≥ 3 cm, thickened/enhancing cyst walls or nonenhancing mural nodules may not necessarily lead to a recommendation for surgical resection but can suggest the performance of endoscopic ultrasound (EUS) guided fine needle aspiration (11).

With regard to the primary diagnostic modality for the evaluation of IPMNs, CT and MR imaging are both currently recommended as primary diagnostic imaging tests for the evaluation of IPMNs according to the International consensus guidelines 2012 (11) whereas MR imaging with MR cholangiopancreatography (MRCP) is recommended for the characterization and follow-up of pancreatic cysts according to the American College of Radiology (12). Although several studies

have demonstrated that EUS may in fact be more sensitive than CT or MR imaging, it is an invasive procedure and suffers from interobserver variability (13). Thus, at present, CT is widely used as the primary diagnostic test for the evaluation of focal pancreatic tumors at many institutes owing to its good performance in temporal and spatial resolution as well as its wide availability. MR imaging, on the other hand, has increasingly been used for the evaluation of pancreatic diseases owing to its high-contrast resolution and capability in providing high resolution three dimension (3D) MRCP images, which can provide good information regarding the relationship between cystic lesions and pancreatic ductal structures or Intraductal lesions (14-17). However, with recent developments in MRI hardware and software, such as the development of phase array coils, parallel imaging techniques, and 3D T1-weighted rapid imaging sequences (18-20), MRI has become more frequently used for the evaluation of the malignant potential of IPMNs, and for serial follow-up. Therefore, CT and MRI are now often interchangeably used to evaluate and follow-up IPMNs (21). Yet, until now, the inter-modality agreement of these two imaging modalities as well as the question of which modality shows

higher inter-observer agreement and provides better diagnostic performance in evaluating malignant potential has not been investigated. Therefore, the purpose of our study is to compare the diagnostic performances of CT and MRI with MRCP in predicting the malignant potential of IPMNs and to evaluate the inter-observer and inter-modality agreements for the imaging features of IPMNs.

MATERIALS AND METHODS

This study was approved by our institutional review board and the requirement for informed consent was waived owing to the retrospective nature of this study.

Patient population

A search of our institution's medical records and pathologic database from January 2010 through November 2013 revealed 131 patients in whom pancreatic IPMN was diagnosed regardless of its subtype (main duct, branch duct, and combined type). The inclusion criteria for our study were as follows: (1) patients with pancreas IPMNs who had undergone curative or palliative surgery at our hospital and (2) patients who had undergone preoperative pancreas protocol MDCT and MRI examinations including MRCP within three months prior to surgery. Among them, we excluded two patients due to the poor imaging quality of MRI (n=1) or a history of previous pancreas surgery (n=1). Finally, a total of 129 patients (77 men, 52 women; mean age, 64.5 years; age range, 12-85 years) comprised our study population. Detailed description of the demographic data for the 129 patients included in our study are summarized in

Table 1.

CT technique

All patients underwent either quadruple-phase MDCT (n=108) consisting of precontrast, early arterial, late arterial (pancreatic), and venous phases, or triple-phase MDCT (n=21) consisting of precontrast, pancreatic, and venous phases. CT scans were obtained using one of the following MDCT scanners: a 320-channel CT scanner (Aquilion one (n=9); Toshiba, Otawara-shi, Japan); a 128 channel CT scanner (Ingenuity (n=4), Philips Healthcare, Best, the Netherlands); a 64-channel scanner (Brilliance (n=64), Philips Healthcare, Best, the Netherlands; Somatom definition (n=16), Siemens Medical Solutions, Erlangen, Germany; Discovery 750 (n=1), GE Medical Systems, Milwaukee, Wis); or a 16-channel CT scanner (Somatom emotion (n=1), Siemens Medical Solutions, Erlangen, Germany; LightSpeed (n=1), GE Medical Systems, Milwaukee, Wis; Sensation 16 (n=33), Siemens Medical Solutions, Erlangen, Germany).

For precontrast phase scanning, images with 2.5 to 3.0

mm thick sections were acquired. A total of 1.5 mL of a nonionic contrast medium (Iopromide [370 mg of iodine per milliliter], Ultravist 370; Schering, Berlin, Germany) per kilogram of body weight was administered using a power injector (Multilevel CT; Medrad, Pittsburgh, Pa) at a rate of 2~5 mL/s with a 18-20 gauge intravenous catheter in the antecubital vein, followed by a 20~30 mL sterile saline flush. For imaging acquisition, an automatic bolus tracking technique was used. The trigger threshold was 100 Hounsfield units at the abdominal aorta. Early arterial phase imaging was obtained 6 seconds after the trigger threshold was achieved and the late arterial phase (pancreatic phase) was obtained 5 to 9 seconds after the early arterial phase. The average scanning time delay was 24 seconds for the early arterial phase, 37-45 seconds for the pancreatic phase and 70 seconds for the venous phase. Parameters for the 16-, 64-, 128-, 320- channel multidetector CT in our institution are as follows: detector configuration, 16 x 0.75, 64 x 0.625, 64 x 0.625, and 160 x 0.5 mm, respectively; section thickness, 2.5-3 mm; reconstruction interval, 2-3 mm; pitch, 1-1.5, 0.9-1.2, 1.17 and 0.813, respectively; effective amperage setting, 80-150, 150-190, 80-120 and 50-180 mAs, respectively; rotation time, 0.5, 0.75,

0.5 and 0.5, respectively; tube voltage, 12 kVp; matrix, 512x512; and field of view, 300-390 (Appendix 1).

MRI with MRCP technique

Various MR machines were used to perform MRI with MRCP owing to the retrospective nature of this study. MR imaging was performed with either a 1.5T MR unit (Signa Excite HDXT, GE Medical Systems, Milwaukee, Wis (n=9); Achieva, Philips Healthcare, Best, the Netherlands (n=7); or Avanto, Siemens Medical Solutions, Erlangen, Germany (n=6)) with an eight-channel phased-array torso coil or a 3T MR unit (Magnetom Verio or Trio, Siemens Medical Solutions, Erlangen, Germany (n=101); or Ingenia, Philips Healthcare, Best, the Netherlands (n=6)) with a 32- or 12-channel phased-array torso coil. All of the MR sequence parameters used for these two scanners are summarized in Appendix 2.

Unenhanced axial, T2-weighted (T2W), T1-weighted (T1W), respiratory-triggered DWI, and coronal MRCP images were obtained prior to contrast injection. T2-weighted imaging was

obtained using a single-shot fast spin-echo sequence or a half-Fourier acquisition single-shot turbo spin-echo sequence with or without fat saturation with the patients requested to perform a breath hold during acquisition, and the T1-weighted gradient-echo sequence was performed with in- and opposed- phase unenhanced fat-saturation images (volume interpolation with breath-hold examinations: VIBE, Siemens Medical Solutions, Germany). Diffusion weighted imaging (DWI) was obtained using a single-shot echo-planar imaging pulse sequence with b values of 0, 400, and 800 sec/㎟ using respiratory triggering. Thin slice MRCP images were reconstructed using a maximum intensity projection algorithm with 3D workstation transformation (Advanced Workstation, GE Medical Systems).

Dynamic fat-saturated, T1W 3D GRE imaging acquisition was performed before and after injection of 1.0M gadobutrol (7.5 mL of Gadovist; Bayer Healthcare, Berlin, Germany) with 0.1 mmol/Kg of body weight at a rate of 2 mL/sec. The average scanning time delay was 8 seconds for the early arterial phase, 60 seconds for the portal phase and 2, 3, 5 and 10 minutes for the delay phase after arrival of the contrast media in the distal

thoracic aorta using the MR fluoroscopic technique. Thereafter, post enhancement subtraction images were obtained in all patients.

Image Analysis

Three radiologists (J.J.H., H.B.Y., and K.H.J, with 6, 6 and 4 years of experience in abdominal imaging, respectively) independently reviewed all MDCT and MRI with MRCP images. They were blinded to the patients' histological diagnosis as well as any clinical or laboratory information, but were aware that the study population had pancreas IPMNs. In order to reduce recall bias, image review of MDCT and MRI with MRCP imaging was done with at least a 2 week interval between reading sessions. The readers reviewed all CT and MRI data sets according to the International consensus guidelines 2012 for the management of IPMN and MCN of pancreas (11), focusing on imaging features of "high-risk stigmata" and "worrisome features". In addition, reviewers also evaluated the presence or absence of "parenchymal mass" and "locoregional extension" of solid lesions associated with IPMN to determine whether those findings can

be used as “overt malignancy signs” similar to “high risk stigmata”, as both parenchymal mass and locoregional extension have been suggested to indicate the presence of invasive cancer associated with IPMN (22). Parenchymal mass was defined as a solid lesion with a different signal or attenuation from that of the adjacent pancreatic parenchyma (Figure 1). Locoregional extension was defined as peripancreatic infiltration or adjacent organ invasion into the duodenum, biliary tree, ampulla of Vater, stomach or spleen.

Recording of findings – According to the International consensus guidelines 2012, a main pancreatic duct (MPD) size larger than 10 mm and an enhancing mural nodule were recorded as “high risk stigmas” and an MPD size ranging from 5-9 mm, a cyst size larger than 30 mm, a nonenhancing mural nodule, a thickened and enhanced cyst wall as well as abrupt pancreatic duct (p-duct) change with parenchyma atrophy were recorded as “worrisome features”.

The largest diameter of cysts was measured on any axial, coronal or sagittal plane on CT and at any axial or coronal image

of the MRCP sequence on MRI. The cutoff value was 30 mm. MPD diameter was measured with an electronic caliper included in the picture archiving and communication system (PACS) program by each of the reviewers and was categorized into one of three categories; smaller than 5 mm, larger than 5 mm but smaller than 10 mm, or larger than 10 mm in diameter, respectively. Mural nodules were defined as any solid nodule in the MPD or the branch duct of a well-circumscribed tissue lesion surrounded by a duct wall (Figure 2). To evaluate mural nodules in cases of IPMNs, we divided them into three categories, no mural nodules, non-enhancing mural nodules and enhancing mural nodules. A thickened and enhanced cyst wall was defined as a cyst wall greater than 2 mm in width with enhancement (Figure 3).

For evaluation of the overall diagnostic performance of both MDCT and MRI in predicting malignancy of IPMNs, we adopted a scoring system utilized in previous studies as follows (23, 24): score 1, no worrisome features or high risk stigmata and definite branch duct type IPMN; score 2, one worrisome feature without high risk stigma; score 3, more than 2 worrisome

features without high risk stigma; score 4, one high risk stigma; and score 5, more than 2 high risk stigmata. IPMNs with a score of 1 are regarded as “low-risk IPMNs”. The diagnostic performance score of preoperative MDCT and MRI with MRCP for prediction of malignancy of IPMNs were compared with the pathology determined WHO grades (23).

Histopathologic Analysis

All resected IPMNs were reviewed by an experienced pathologist (K.B.L., with more than 10 years of experience) according to the 2010 World Health Organization criteria (25). Information of the type of IPMN, WHO grade, location of the tumor, size of the tumor, presence of mural nodules, diameter of the MPD, peripancreatic infiltration, vascular involvement, LN metastasis, perineural invasion, and involvement of adjacent solid organs were determined through pathologic analysis which were routinely described in the pathologic report at our institution. IPMNs were classified into four different histological grades: low grade dysplasia, intermediate grade dysplasia, high grade dysplasia, and invasive cancer (6). Among cases of IPMN with

invasive cancers, the diagnosis of ductal adenocarcinoma associated with IPMN was additionally made when it possessed an invasive component of greater than 50% with morphologic characteristics of a tubular carcinoma and an intraductal component with a micropapillary structure showing dysplasia (26). In this study, low grade dysplasia and intermediate grade dysplasia were classified as nonmalignant, while high grade dysplasia and invasive cancers were regarded as malignant as described in previous studies (23, 27).

Statistical analysis

The prevalence of enhancing mural nodules, MPD diameter (≥ 10 mm or 5-9 mm), cyst size, abrupt MPD change with parenchymal atrophy, a thickened and enhancing cyst wall, parenchymal mass and locoregional extension were analyzed using the χ^2 test and the presence of non-enhancing mural nodules and lymphadenopathy were analyzed using Fisher's exact test with commercially available statistical software (SPSS, version 21; SPSS, Chicago, Ill). Sensitivity, specificity and area

under the curve (AUC) values were calculated at both CT and MRI with MRCP for the prediction of the malignant potential of IPMN and for the prediction of invasive cancer. Interobserver agreements and consistency between imaging modalities were assessed using weighted κ statistics for noncontinuous scales and with the intraclass correlation coefficient (ICC) for continuous scales using commercially available statistical software (Medcalc, version 14.8.1.0; MedCalc, Marikerke, Belgium). The strength of agreement was evaluated as follows: a κ value and ICC value of less than 0.20 indicated poor agreement; 0.21-0.40, fair agreement; 0.41-0.60, moderated agreement; 0.61-0.80, good agreement; and 0.81-1.0, excellent agreement.

RESULTS

Interobserver agreement for each stigmata sign and worrisome feature on MDCT and MRI with MRCP

All the stigmata and worrisome features except for a thickened and enhanced cyst wall and lymphadenopathy showed moderate to good interobserver agreement on both CT and MRI (Table 2). More specifically, the three readers showed excellent agreement in measuring cyst size (κ=0.87-0.94 for CT, κ=0.92-0.95 for MRI) and MPD diameter (ICC=0.91 for CT, ICC=0.91 for MRI), and good agreement for mural nodule character (ICC=0.73 for CT, ICC=0.80 for MRI). However, the assessment of lymphadenopathy (κ=0.30-0.40 for CT, κ=0.38-0.66 for MRI) and an enhanced cyst wall (κ=0.15-0.29 for CT, κ=0.17-0.31 for MRI) showed only poor to fair agreement.

Inter-modality agreement between MDCT and MRI with MRCP

Malignant features. – MDCT and MRI with MRCP showed excellent agreement with regard to MPD size (ICC=0.97) and good agreement in evaluating enhancing mural nodules (κ=0.70) (Figure 2). In addition, in the evaluation parenchymal mass and locoregional extension, both

MDCT and MRI showed excellent agreement (κ=0.81 and 0.81), respectively (Table 3).

Worrisome features. – MDCT and MRI with MRCP showed excellent agreement for lymphadenopathy (κ=1.00) and abrupt change of MPD with distal parenchyma atrophy (κ=0.95). In addition, with regard to the detection of mural nodules (κ=0.65), cyst size (κ=0.58) and the presence of a thickened and enhancing cyst wall (κ=0.57), the inter-modality agreement showed moderate to good agreement (Table 3).

Diagnostic performance of MDCT and MRI in predicting the malignant potential of IPMNs

Prediction of high grade dysplasia. – The overall diagnostic performance of both MDCT and MRI was similar (AUC value; reader 1, 0.76 vs. 0.79; reader 2, 0.76 vs. 0.77; reader 3, 0.82 vs. 0.82) in predicting the malignant potential with good inter-modality agreement (k=0.75). In addition, MDCT and MRI with MRCP both showed moderate interobserver agreement in predicting the malignant potential of IPMNs between the three readers (κ=0.47-0.53 for CT, κ=0.51-0.59 for MRI) (Table 4 and Figure 4).

Prediction of invasive IPMN. – Similar to the results of malignant potential prediction of high grade dysplasia, the overall diagnostic

performance of MDCT and MRI with MRCP were similar (AUC value: reader 1, 0.67 vs. 0.69; reader 2, 0.69 vs. 0.69; reader 3, 0.77 vs. 0.75) (Table 4). However, after including the presence of parenchymal mass and locoregional extension as overt malignancy signs similar to “high risk stigmata”, the diagnostic performances of MDCT and MRI with MRCP (AUC value: reader 1, 0.77 vs. 0.78; reader 2, 0.83 vs. 0.85; reader 3, 0.87 vs. 0.88) were higher than those of the AUC value (reader 1, 0.65 vs. 0.68; reader 2, 0.67 vs 0.67; reader 3, 0.77 vs. 0.73) based on the International consensus guidelines 2012, resulting in higher sensitivity (94.3% vs 70.2% for CT, and 94.3% vs. 71.4% for MRI) and equivocal specificity (69.1% vs 70.2% for CT and 71.3% vs. 72.3% for MRI) (Table 4).

Age, years (range)	64.5 (12-85)
Sex	
Male	77 (59.7%)
Female	52 (40.3%)
IPMN type	
MPD	16 (12.4%)
Branch duct	47 (36.4%)
Combined	49 (38.0%)
Unclassified	17 (13.2%)
Location	
Uncinate	49 (38.0%)
Head	40 (31.0%)
Neck	22 (17.1%)
Body	45 (34.9%)
Tail	40 (31.0%)
Pathologic grade	
Benign	70 (54.3%)
High grade dysplasia (In situ)	24 (18.6%)
Invasive	35 (27.1%)
Operation	
PPPD	68 (52.7%)
Distal pancreatectomy	44 (34.1%)
Total pancreatectomy	5 (3.9%)
Others	12 (9.3%)

Table 1. Patient demographic data

Imaging findings	CT				MR			
	Benign IPMN (N=70)	Malignant IPMN (N=59)	ρ-value*	Interobserver agreement †	Benign IPMN (N=70)	Malignant IPMN (N=59)	ρ-value*	Interobserver agreement†
High-risk stigma								
MPD diameter ≥ 10mm	10 (14.3)	25 (42.4)	<.001	ICC = 0.91	9 (12.9)	24 (40.1)	<.001	ICC = 0.91
Enhancing mural nodule	5 (7.1)	34 (56.6)	<.001	ICC = 0.73	4 (5.7)	31 (52.5)	<.001	ICC = 0.80
Worrisome feature								
Cyst size ≥ 30mm	20 (28.6)	36 (61.0)	<.001	0.94, 0.87, 0.87	31 (44.3)	34 (57.6)	0.158	0.94, 0.95, 0.92
MPD diameter 5-9mm	23 (32.9)	22 (37.2)	<.001	ICC = 0.91	23 (32.9)	23 (40.0)	<.001	ICC = 0.91
Non-enhancing mural nodule	4 (5.7)	0 (0)	<.001	ICC = 0.73	4 (5.7)	2 (3.4)	<.001	ICC = 0.80
Abrupt caliber change	5 (7.1)	18 (30.5)	<.001	0.53, 0.34,0.49	6 (8.6)	19 (32.2)	<.001	0.55, 0.36, 0.41
Enhanced cyst wall	18 (25.7)	25 (42.4)	0.061	0.15, 0.29, 0.20	21 (30.0)	32 (54.2)	0.007	0.20, 0.31, 0.17
Lymphadenopathy	0 (0)	4 (6.8)	0.041	0.40, 0.35, 0.30	0(0)	4 (6.8)	0.041	0.38, 0.43, 0.66
Parenchymal mass	1 (1.4)	19 (32.2)	<.001	0.33, 0.51, 0.61	1 (1.4)	24 (40.7)	<.001	0.28, 0.24, 0.57
Locoregional extension	0 (0)	23 (39.0)	0.001	0.53, 0.51, 0.79	0 (0)	22 (37.3)	0.001	0.35, 0.40, 0.60

Table 2. Differences in imaging features between benign IPMNs and malignant IPMNs

Unless otherwise indicated, data are numbers of patients and data in parentheses are percentage.

* Determined with Fisher exact test and chi square test

† Unless otherwise indicated, data are **κ value** and serially noted reader 1 &2, 1&3 and 2&3 agreement.

	Inter-modality consistency
MPD diameter	ICC=0.97
Mural nodule	ICC=0.82
Nodule detection	0.65
Nodule enhancement	0.70
Size	0.58
Thickened and enhanced cyst wall	0.57
Abrupt caliber change with distal atrophy	0.95
Lymphadenopathy	1.00
Parenchymal mass	0.81
Locoregional extension	0.81

Table 3. Inter-modality agreements between CT and MRI of the high risk stigmatas and worrisome features

Unless otherwise indicated, data are κ value.

	MDCT				MR with MRCP				Intermodality agreement†
	Sensitivity	Specificity	AUC*	Interobserver agreement†	Sensitivity	Specificity	AUC*	Interobserver agreement†	
Diagnosis of malignant IPMNs									
Original guideline	69.5	81.4	0.82	0.47-0.53	67.8	84.3	0.82	0.51-0.59	0.75
Addition of parenchyma mass and locoregional extension	81.4	80	0.87	0.57-0.61	81.4	82.9	0.89	0.54-0.65	0.77
Diagnosis of invasive IPMN									
Original guideline	74.3	70.2	0.77	0.47-0.53	71.4	72.3	0.75	0.51-0.59	0.75
Addition of parenchyma mass and locoregional extension	94.3	69.1	0.87	0.57-0.61	94.3	71.3	0.88	0.54-0.65	0.77

Table 4. Diagnostic performance of CT and MR in prediction of malignant potential

Unless otherwise indicated, sensitivity and specificity data are percentage.

* AUC = area under the curve value

† Unless otherwise indicated, data are κ value.

(A)

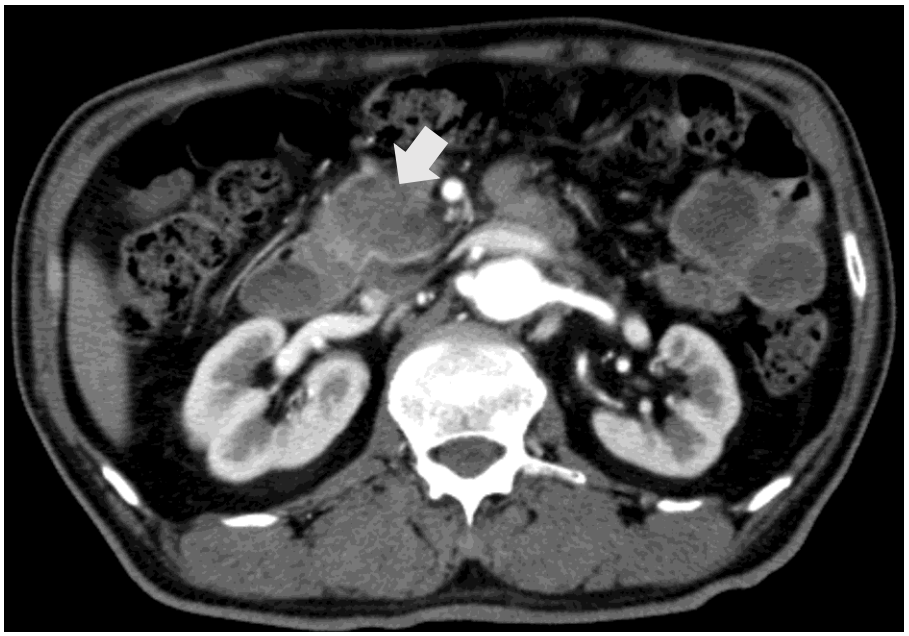

(B)

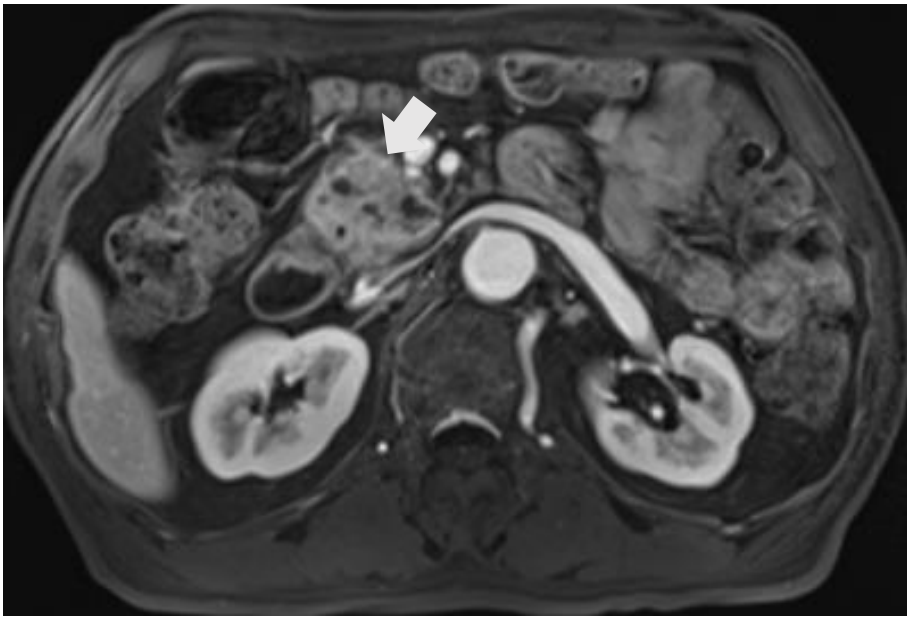

(C)

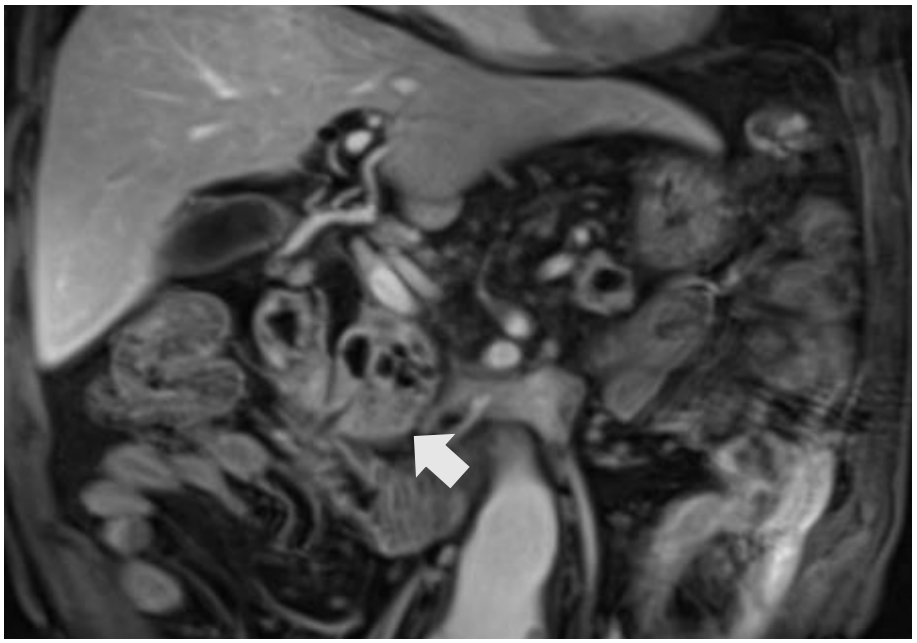

(D)

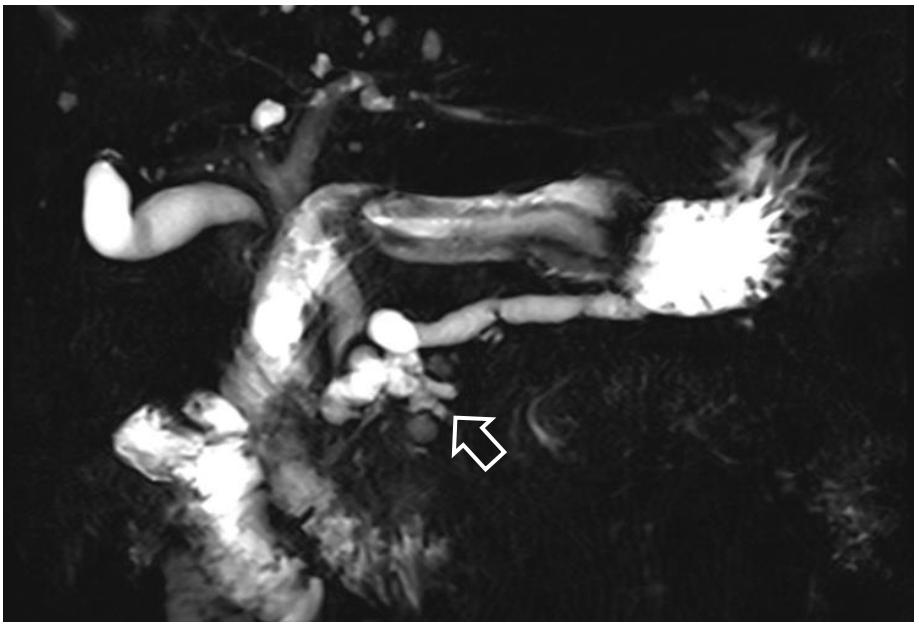

Figure 1. Parenchymal mass on MDCT and MR with MRCP

A 67 year old male with confirmed invasive IPMN on surgical specimen. On preoperative axial CT image (A), a 37 mm, ill-defined, low attenuating parenchyma mass (arrow) is observed. On MRI, a hypoenhancing parenchyma mass (arrow) abutting dilated branch ducts can be seen in the 3 min delayed axial (B) and coronal images (C). MRCP shows a multiloculated cystic lesion at the pancreas head (black arrow) as well as dilatation of the main pancreatic duct (D).

(A)

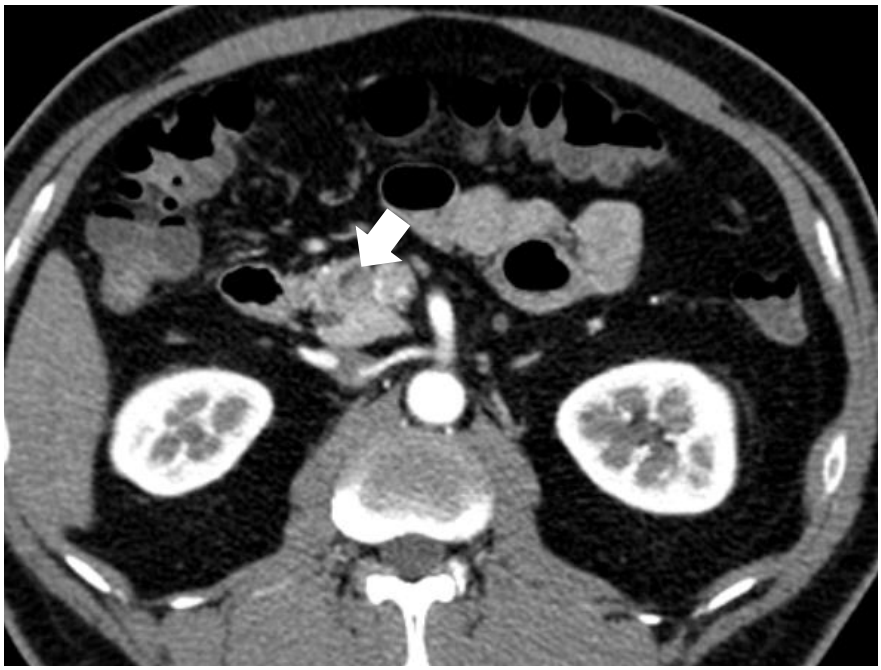

(B)

(C)

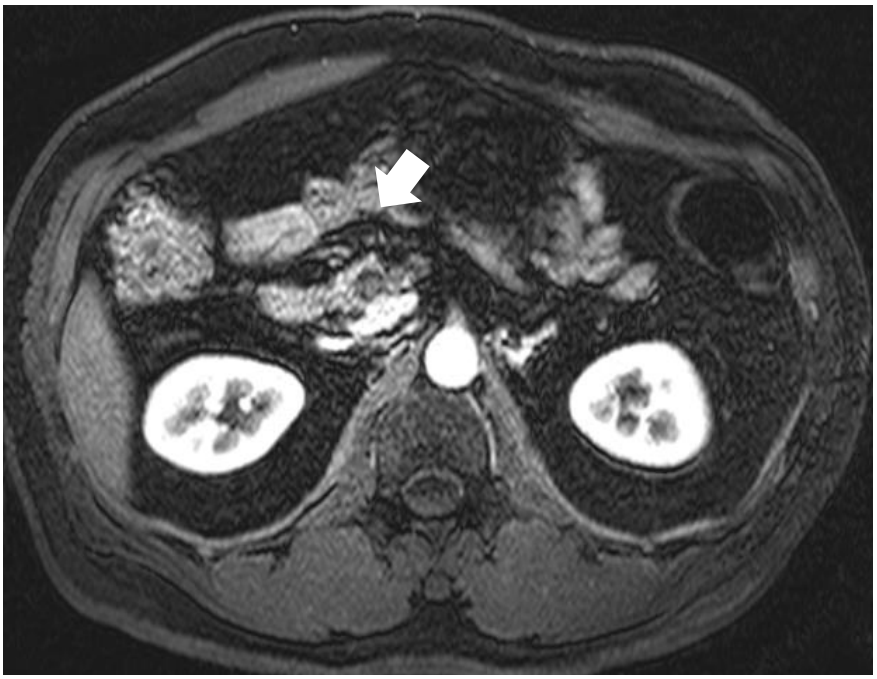

(D)

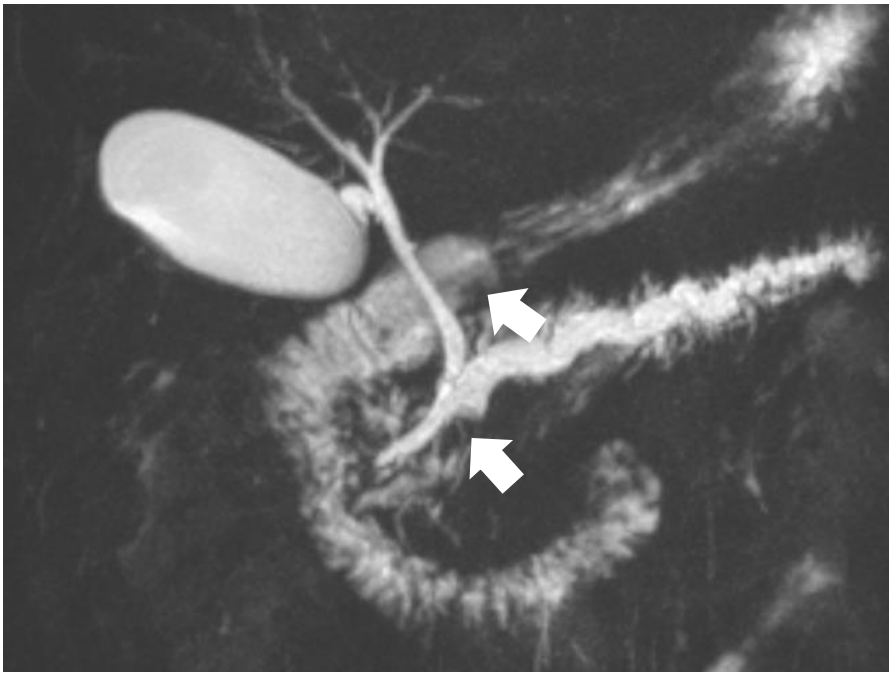

Figure 2. Mural nodule on MDCT and MR with MRCP

A 50 year old male with confirmed main duct type high grade dysplasia IPMN on surgical specimen. On preoperative axial and coronal CT images (A, B), a 5 mm enhancing mural nodule in the main pancreatic duct (arrow) can be observed. On MRI, the intra-ductal enhancing mural nodule (arrow) is also well demonstrated on the axial T1-weighted image during arterial phase (C). MRCP shows an intraluminal filling defect (arrow) as well as dilatation of the upstream main pancreatic duct (D).

(A)

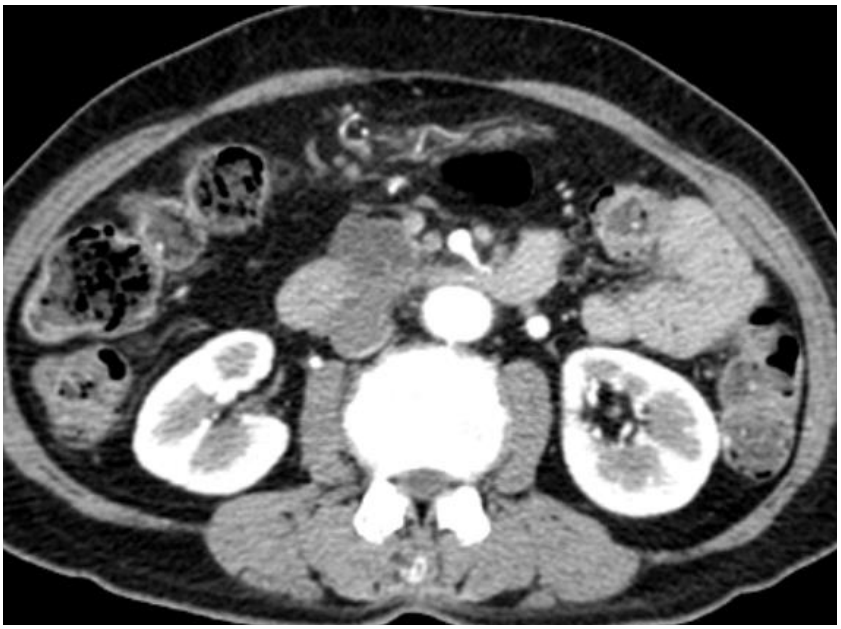

(B)

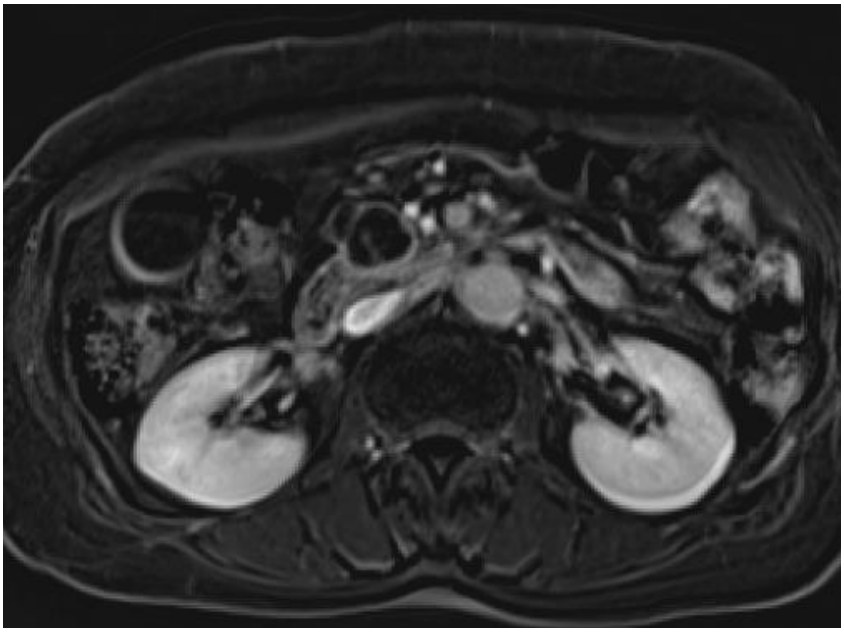

(C)

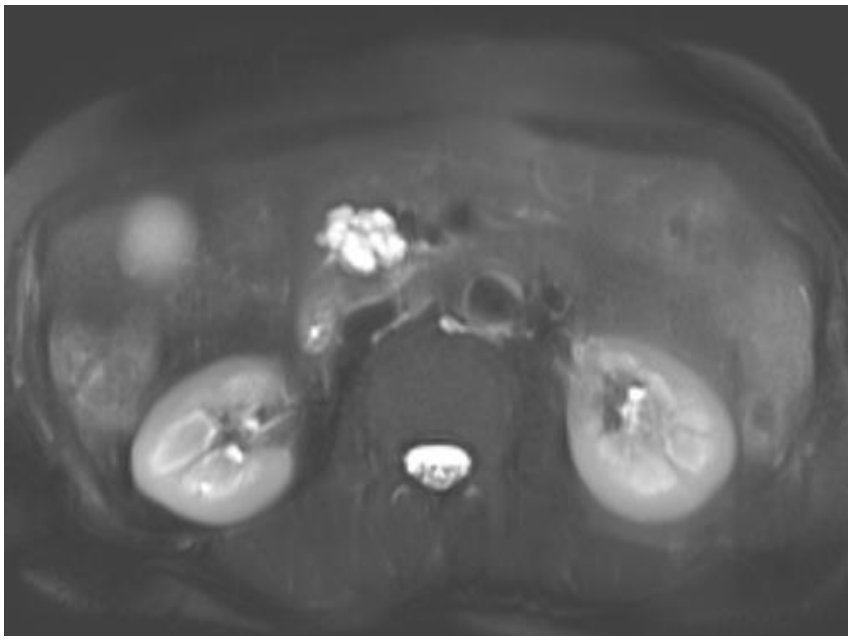

(D)

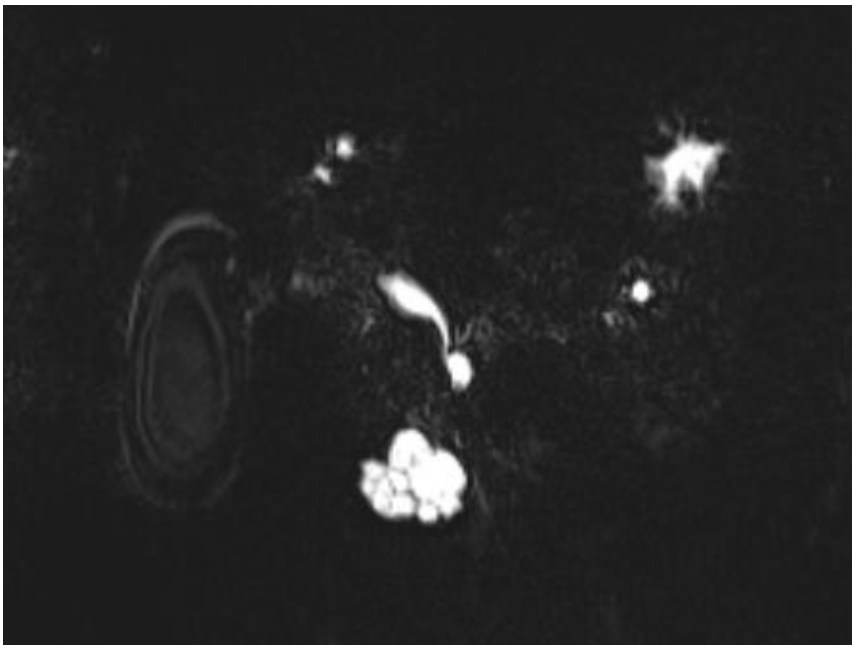

Figure 3. Thickened and enhanced cyst wall on MDCT and MR with MRCP

A 69 year old female with confirmed invasive IPMN on surgical specimen. On preoperative CT image (A), a 2 mm thick enhancing septum in a multilocuated cyst (arrow) is observed. On MRI, the subtraction image of arterial phase scan (B) and the heavily T2-weighted image (C) shows the septal enhancement and thickened septum more visibly. MRCP shows a multiloculated cystic lesion at the pancreas head (arrow) (D).

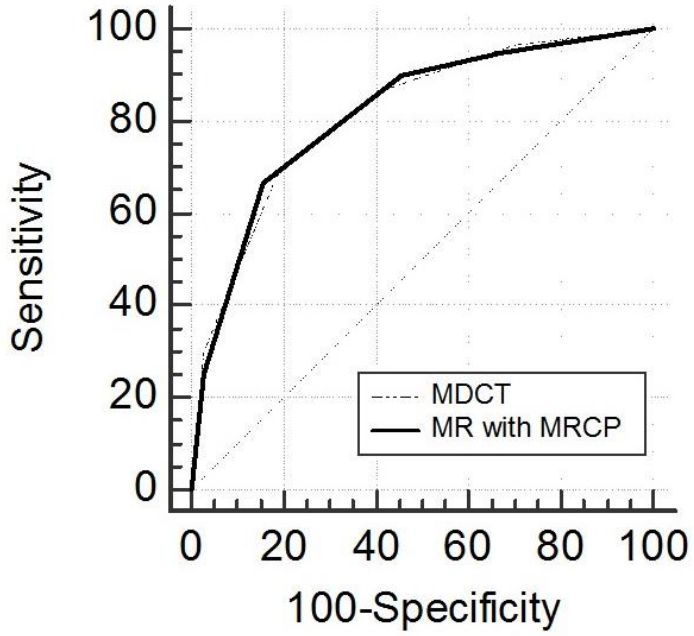

Figure 4. AUC comparison between MDCT and MR with MRCP

Both MDCT and MR with MRCP showed high consistency to prediction of IPMN malignant potential (k=0.75) with moderate interobserver agreement (κ=0.47-0.53 in CT, κ=0.51-0.59 in MR). The cut off score is 3 which means more than 2 worrisome features without high risk stigmatas.

DISCUSSION

With the increasing incidental detection rate of IPMNs on abdominal CT or MRI in clinical practice today, the prediction of their malignant potential so as to avoid unnecessary surgical interventions and to potentially treat malignant lesions at an early stage has become even more important (28). With this in mind, the International consensus guidelines 2012 for the management of IPMNs and MCNs of the pancreas (11) was recently developed. In this guideline, they stratified the findings of the patients into two clinical categories, "high-risk stigmata" and "worrisome features," and recommended different therapeutic strategies based on these findings (24). In our study, the diagnostic performances of MDCT and MRI in predicting overall malignant potential using the criteria provided by the guidelines were quite comparable (AUC value; reader 1, 0.76 vs. 0.79; reader 2, 0.76 vs. 0.77; reader 3, 0.82 vs. 0.82) with good inter-modality agreement (κ=0.75) and moderate interobserver agreement (κ=0.47-0.53 for CT, κ=0.51-0.59 for MRI) when we set high grade dysplasia as the cutoff for malignancy. Likewise, in the prediction of invasive IPMNs, MDCT and MRI also

demonstrated similar predictability (AUC value: reader 1, 0.67 vs. 0.69; reader 2, 0.69 vs. 0.69; reader 3, 0.77 vs. 0.75) with good inter-modality agreement (κ = 0.75) and moderate interobserver agreement (κ=0.47-0.53 for CT, κ=0.51-0.59 for MRI) (Table 4).

We also found in our study that the inter-modality agreement of each of the stigmata signs and worrisome features between MDCT and MRI was good (k= 0.57~1.0); evaluation of lymphadenopathy (κ=1.00) showed the highest consistency followed by abrupt MPD caliber change with distal pancreas parenchymal atrophy (κ=0.95). In addition, measurement of the MPD diameter (ICC=0.97) and characterization of mural nodules (ICC=0.82) also presented high consistency. The least consistent imaging finding was the evaluation of a thickened and enhancing cyst wall which was more frequently detected by MRI than MDCT (Table 3). However, this may be explained by the high tissue contrast capability provided by the dynamic subtraction sequence of MRI and MRCP, making it easier to interpret subjectively (Figure 3).

As for the interobserver agreement of each of the stigmata signs and worrisome features on CT and MRI, we found that

there was good agreement overall (Table 2). On MDCT, evaluation of cyst size (κ=0.87-0.94) presented the highest agreement followed by locoregional extent (κ=0.51-0.79). Measurement of the MPD diameter (ICC=0.91) also showed high agreement. The poorest agreement was found in the determination of a thickened and enhancing cyst wall (κ=0.15-0.29). On MRI, the highest agreement was observed for the evaluation of cyst size (κ=0.92-0.95) followed by lymphadenopathy (κ=0.38-0.66). In addition, similar to the MDCT findings, a thickened and enhancing cyst wall (κ=0.17-0.31) showed the poorest agreement on MRI. As was the case in the assessment of inter-modality agreement, this may be due to the fact that detecting a thickened and enhancing cyst wall can be quite subjective (Figure 3). The high interobserver agreement of each stigmata and worrisome feature is meaningful because evaluation of pancreas cystic lesions has previously been shown to be quite variable between radiologists. Indeed, previous studies have shown that this variance in evaluation has led to confusing treatment planning and unnecessarily increased health care cost in the past (9, 29-31). We believe that the high interobserver agreement in each imaging finding, except for

determination of a thickened and enhancing cyst wall, in our study could be attributed to the improved image quality of MDCT and MRI owing to recent technological developments which now allow higher temporal and spatial resolution.

Given that CT has advantages over MRI with MRCP in terms of spatial resolution and wider availability (29, 32-34) whereas MRCP is more useful in evaluating ductal communication and ductal abnormalities than CT (12), at many institutes, both modalities are equally used for the evaluation of IPMNs, and interchangeably used for the follow-up of IPMNs. Although several previous studies have demonstrated that both CT and MRI can be useful in determining the malignant potential of IPMNs (21, 29, 35-40), until now, there have been no studies that have assessed the inter-modality agreement for determining stigmata signs and worrisome features on CT or MRI. Based on our study results which showed good inter-modality agreements between MDCT and MRI, we believe that MDCT and MRI can be interchangeably used for the evaluation of the malignant potential of IPMNs as well as for follow-up. In cases of IPMNs with no worrisome features or only one worrisome feature

(scores 1 and 2), however, follow-up with MRI is more highly recommended considering the radiation hazard of CT (12, 41).

Finally, we also considered features of “parenchymal mass” and “locoregional extension”, which may represent advanced stage features of invasive cancer, as “overt malignancy signs” similar to “high risk stigmata”, and found that the invasive IPMN predictability was significantly increased (AUC: 0.87 in CT, 0.88 in MRI) with high sensitivity (94.3%) and equivocal specificity (69.1%)(Table 4). These features also provided high inter-modality agreement (κ = 0.77) and moderate to good interobserver agreement (κ=0.57-0.61 in CT, κ=0.54-0.65 in MRI). Several previous studies have demonstrated that an increase in the number of predictive factors can augment the determination of the likelihood of malignancy in branch duct IPMNs (25, 42, 43). Considering that these imaging features of parenchymal mass and locoregional extension can represent an invasive component with morphologic characteristics of a tubular or colloid carcinoma in the pancreas parenchyma or peripancreatic infiltration of advanced stage IPMN-associated invasive cancers, we believe that they should potentially be considered for inclusion as a

“high-risk stigmata” in future guidelines.

Our study has several limitations. First, owing to the retrospective nature of this study, there may have been unavoidable selection bias. However, in our institution, a large number of patients with IPMNs underwent both MDCT and MRI for preoperative evaluation, and thus the selection bias may have been minimal. Second, MDCT and MRI were obtained using different scanners although we used similar imaging parameters for dynamic imaging and MRCP.

In conclusion, the overall diagnostic performances of MDCT and MRI with MRCP for the prediction of pancreas IPMN malignancies was shown to be similar, suggesting that interchangeable follow-up may be possible. In addition, inclusion of “parenchymal mass” and “locoregional extension” as additional “overt malignant signs” similar to “high risk stigmata” was shown to increase overall diagnostic performance with higher sensitivity without a significant decrease in specificity.

.

Appendix

Scanners*	DC (mm)	ST (mm)	RI (mm)	Pitch	Tube current (mAs)	RT (sec)	Tube voltage (kVp)	Matrix	FOV (mm)
16	16x0.75	3	2-3	1-1.5	80-160	0.5	120	512x512	300–390
64	64x0.625	2.5-3	2-3	0.9-1.2	150-190	0.75	120	512x512	300–390
128	64x0.625	3	2	1.172	80-120	0.5	120	512x512	300–390
320	160x0.5	3	2	0.813	50-180	0.5	120	512x512	300–390

Appendix 1. CT parameters

* Numbers are channels.

DC= detector collimation; ST= slice thickness; RI =reconstruction interval; RT= rotation time; FOV=field of view.

Parameter	T1WI		T2WI		DWI		3D MRCP		Dynamic image	
	1.5T	3.0T	1.5T	3.0T	1.5T	3.0T	1.5T	3.0T	1.5T	3.0T
TR (msec) /TE (msec)	4.6/2.2	6.6/2.1	850/99	1553.7/80	6000/59.6	1311/66	850/161	2576/740	4.6/2.2	4.5/2.2
FA (degree)	12	10	90	90	90	90	90	90	12	10
Thickness(mm)	4.8	6	7	7	7	7	3	2	4.8	6
Matrix	320x192	320x222	320x192	380x365	128x128	128x102	320x192	320x318	320x192	332x291
FOV (mm)	350	379	350	380	400	399	350	350	350	379
ETL	1	1	1	99	1	27	1	160	1	1

Appendix 2. MR parameters

T1WI = T1-weighted images; T2WI = T2-weighted images; DWI = diffusion-weighted images; MRCP = magnetic resonance cholangiopancreatography; 3D = three-dimensional; TR = repetition time; TE = echo time; FA = flip angle; FOV = field of view; ETL = echo train length.

References

1. Sohn TA, Yeo CJ, Cameron JL, Iacobuzio-Donahue CA, Hruban RH, Lillemoe KD. Intraductal papillary mucinous neoplasms of the pancreas: an increasingly recognized clinicopathologic entity. Ann Surg. 2001;234(3):313.
2. Reid-Lombardo KM, St Sauver J, Li Z, Ahrens WA, Unni KK, Que FG. Incidence, Prevalence, and Management of Intraductal Papillary Mucinous Neoplasm in Olmsted County, Minnesota, 1984–2005 A Population Study. Pancreas. 2008;37(2):139.
3. de Beeck BO, Spinhoven M, Corthouts B, de Jongh K, Salgado R, Parizel P. Management of cystic pancreatic masses. JBR-BTR. 2007;90(6):482-6.
4. Freeny PC, Saunders MD. Moving beyond morphology: new insights into the characterization and management of cystic pancreatic lesions. Radiology. 2014;272(2):345-63.
5. Hruban RH, Takaori K, Klimstra DS, et al. An illustrated consensus on the classification of pancreatic intraepithelial neoplasia and intraductal papillary mucinous neoplasms. Am J Surg Pathol. 2004;28(8):977-87.
6. Bosman FT, Carneiro F, Hruban RH, Theise ND. WHO classification of tumours of the digestive system: World Health

Organization, 2010.

7. Sohn TA, Yeo CJ, Cameron JL, et al. Intraductal papillary mucinous neoplasms of the pancreas: an updated experience. Ann Surg. 2004;239(6):788.

8. Hruban R, Pitman MB, Klimstra D. Tumors of the Pancreas, Afip Atlas of Tumor Pathology, 4th Series Fascicle 6. American Registry of Pathology, Washington DC. 2007. p.252-4.

9. Macari M, Megibow AJ. Focal cystic pancreatic lesions: variability in radiologists' recommendations for follow-up imaging. Radiology. 2011;259(1):20-3.

10. Ip IK, Mortele KJ, Prevedello LM, Khorasani R. Focal cystic pancreatic lesions: assessing variation in radiologists' management recommendations. Radiology. 2011;259(1):136-41.

11. Tanaka M, Fernandez-del Castillo C, Adsay V, et al. International consensus guidelines 2012 for the management of IPMN and MCN of the pancreas. Pancreatology : official journal of the International Association of Pancreatology. 2012;12(3):183-97.

12. Berland LL, Silverman SG, Gore RM, et al. Managing incidental findings on abdominal CT: white paper of the ACR incidental findings committee. J Am Coll Radio.

2010;7(10):754-73.

13. Tanaka M. Controversies in the management of pancreatic IPMN. Nature Rev Gastroenterol Hepatol. 2011;8(1):56-60.

14. SH Y, JM L, JY C, et al. Small (< 20 mm) Pancreatic Adenocarcinomas: Analysis of Enhancement Patterns and Secondary Signs with Multiphasic Multidetector CT. Radiology. 2011;259(2):442-52.

15. K B, KA B, DG T, SP K, B M, A H. Surgically proved visually isoattenuating pancreatic adenocarcinoma undetected in both dynamic CT and MRI. Was blind pancreaticoduodenectomy justified? Int J Surg Case Rep. 2013;4(5):466-9.

16. JH K, SH P, ES Y, et al. Visually Isoattenuating Pancreatic Adenocarcinoma at Dynamic-Enhanced CT: Frequency, Clinical and Pathologic Characteristics, and Diagnosis at Imaging Examinations. Radiology. 2010;257(1):87-96.

17. KM K, JM L, JH Y, B K, JK H, BI C. Intravoxel incoherent motion diffusion-weighted MR imaging for characterization of focal pancreatic lesions. Radiology. 2014;270(2):444-53.

18. Kang KM, Lee JM, Shin CI, et al. Added value of diffusion-weighted imaging to MR cholangiopancreatography with unenhanced MR imaging for predicting malignancy or invasiveness of intraductal papillary mucinous neoplasm of the

pancreas. J Magn Reson Imaging. 2013;38(3):555-63.

19. Park HS, Lee JM, Choi HK, Hong SH, Han JK, Choi BI. Preoperative evaluation of pancreatic cancer: comparison of gadolinium-enhanced dynamic MRI with MR cholangiopancreatography versus MDCT. J Magn Reson Imaging. 2009;30(3):586-95.

20. Yoon LS, Catalano OA, Fritz S, Ferrone CR, Hahn PF, Sahani DV. Another dimension in magnetic resonance cholangiopancreatography: comparison of 2- and 3-dimensional magnetic resonance cholangiopancreatography for the evaluation of intraductal papillary mucinous neoplasm of the pancreas. J Comput Assist Tomogr. 2009;33(3):363-8.

21. Waters JA, Schmidt CM, Pinchot JW, et al. CT vs MRCP: optimal classification of IPMN type and extent. J Gastrointest Surg. 2008;12(1):101-9.

22. Ogawa H, Itoh S, Ikeda M, Suzuki K, Naganawa S. Intraductal Papillary Mucinous Neoplasm of the Pancreas: Assessment of the Likelihood of Invasiveness with Multisection CT 1. Radiology. 2008;248(3):876-86.

23. Kim SH, Lee JM, Lee ES, et al. Intraductal Papillary Mucinous Neoplasms of the Pancreas: Evaluation of Malignant Potential and Surgical Resectability by Using MR Imaging with MR

Cholangiography. Radiology. Epub 2014; DOI: 10.1148/radiol.14132960.

24. Aso T, Ohtsuka T, Matsunaga T, et al. "High-risk stigmata" of the 2012 international consensus guidelines correlate with the malignant grade of branch duct intraductal papillary mucinous neoplasms of the pancreas. Pancreas. 2014;43(8):1239-43.

25. Jang JY, Park T, Lee S, et al. Validation of international consensus guidelines for the resection of branch duct-type intraductal papillary mucinous neoplasms. Br J Surg. 2014;101(6):686-92.

26. Kang MJ, Lee KB, Jang J-Y, et al. Disease Spectrum of Intraductal Papillary Mucinous Neoplasm With an Associated Invasive Carcinoma: Invasive IPMN Versus Pancreatic Ductal Adenocarcinoma-Associated IPMN. Pancreas. 2013;42(8):1267-74.

27. Tamura K, Ohtsuka T, Ideno N, et al. Treatment strategy for main duct intraductal papillary mucinous neoplasms of the pancreas based on the assessment of recurrence in the remnant pancreas after resection: a retrospective review. Ann Surg. 2014;259(2):360-8.

28. Anand N, Sampath K, Wu BU. Cyst features and risk of malignancy in intraductal papillary mucinous neoplasms of the

pancreas: a meta-analysis. Clin Gastroenterol Hepatol. 2013;11(8):913-21.

29. Longnecker DS, Adsay NV, Fernandez-del Castillo C, et al. Histopathological diagnosis of pancreatic intraepithelial neoplasia and intraductal papillary-mucinous neoplasms: interobserver agreement. Pancreas. 2005;31(4):344-9.

30. de Jong K, Nio CY, Mearadji B, et al. Disappointing interobserver agreement among radiologists for a classifying diagnosis of pancreatic cysts using magnetic resonance imaging. Pancreas. 2012;41(2):278-82.

31. Ip IK, Mortele KJ, Prevedello LM, Khorasani R. Focal cystic pancreatic lesions: assessing variation in radiologists' management recommendations. Radiology. 2011;259(1):136-41.

32. Soriano A, Castells A, Ayuso C, et al. Preoperative staging and tumor resectability assessment of pancreatic cancer: prospective study comparing endoscopic ultrasonography, helical computed tomography, magnetic resonance imaging, and angiography. Am J Gastroenterol. 2004;99(3):492-501.

33. Waters JA, Schmidt CM, Pinchot JW, et al. CT vs MRCP: optimal classification of IPMN type and extent. J Gastrointest Surg. 2008;12(1):101-9.

34. Brennan DD, Zamboni GA, Raptopoulos VD, Kruskal JB. Comprehensive Preoperative Assessment of Pancreatic Adenocarcinoma with 64-Section Volumetric CT 1. Radiographics. 2007;27(6):1653-66.

35. Sahani DV, Kadavigere R, Blake M, Fernandez-del Castillo C, Lauwers GY, Hahn PF. Intraductal Papillary Mucinous Neoplasm of Pancreas: Multi–Detector Row CT with 2D Curved Reformations—Correlation with MRCP 1. Radiology. 2006;238(2):560-9.

36. Pedrosa I, Boparai D. Imaging considerations in intraductal papillary mucinous neoplasms of the pancreas. World J Gastrointest Surg. 2010;2(10):324.

37. Vullierme M-P, Giraud-Cohen M, Hammel P, et al. Malignant Intraductal Papillary Mucinous Neoplasm of the Pancreas: In Situ versus Invasive Carcinoma—Surgical Resectability 1. Radiology. 2007;245(2):483-90.

38. Manfredi R, Graziani R, Motton M, et al. Main Pancreatic Duct Intraductal Papillary Mucinous Neoplasms: Accuracy of MR Imaging in Differentiation between Benign and Malignant Tumors Compared with Histopathologic Analysis 1. Radiology. 2009;253(1):106-15.

39. Kawamoto S, Lawler LP, Horton KM, Eng J, Hruban RH,

Fishman EK. MDCT of intraductal papillary mucinous neoplasm of the pancreas: evaluation of features predictive of invasive carcinoma. Am J Roentgenol. 2006;186(3):687-95.

40. Kawamoto S, Horton KM, Lawler LP, Hruban RH, Fishman EK. Intraductal Papillary Mucinous Neoplasm of the Pancreas: Can Benign Lesions Be Differentiated from Malignant Lesions with Multidetector CT? 1. Radiographics. 2005;25(6):1451-68.

41. Campbell NM, Katz SS, Escalon JG, Do RK. Imaging patterns of intraductal papillary mucinous neoplasms of the pancreas: An illustrated discussion of the International Consensus Guidelines for the Management of IPMN. Abdom Imaging. 2014:1-15.

42. Ohtsuka T, Kono H, Nagayoshi Y, et al. An increase in the number of predictive factors augments the likelihood of malignancy in branch duct intraductal papillary mucinous neoplasm of the pancreas. Surgery. 2012;151(1):76-83.

43. Kim KW, Park SH, Pyo J, et al. Imaging features to distinguish malignant and benign branch-duct type intraductal papillary mucinous neoplasms of the pancreas: a meta-analysis. Ann Surg. 2014;259(1):72-81.

국문 초록

목적: 췌장 담관 내 유두 종양의 악성도를 예측하는데 있어서 다중 검출기 전산화 단층 촬영과 자기 공명 담도 췌관 조영술을 포함한 자기 공명 영상의 진단 성능 비교와 장비간 (inter-modality) 일치도를 평가하는데 있다.

대상 및 방법: 병리로 확인된 129명의 췌장 담관 내 유두 종양 환자를 대상으로 3명의 판독의가 각각 독립적으로 수술 전 다중 검출기 전산화 단층 촬영과 자기 공명 담도 췌관 조영술을 포함한 자기 공명 영상의 영상 소견을 평가하였다. 전산화 단층 촬영과 자기 공명 영상에서의 고 위험 징표 (high-risk stigmata)와 위험 소견 (worrisome feature)의 장비간(inter-modality) 일치도와 관측자간 일치도를 분석하였다. 또한 유력한 악성 소견으로 생각되는 실질 종괴와 병변 주변부 침윤의 진단가치를 함께 분석하였다. 진단 성능과 장비 간 (inter-modality) 일치도는 리시버 오퍼레이팅 커브 분석 (receiver operating curves)과 웨이티드 카파 (weighted κ) 통계를 이용하였다.

결과: 고도 형성 이상 (High-grade dysplasia) 이상의 췌장 담관 내 유두 종양의 악성도를 평가하는데 있어 전체적인 예측 성능은 전산화 단층 촬영과 자기 공명 영상이 매우 유사한 값을 보였으며 (곡선하 면적 (AUC): 0.82, 0.82) 높은 장비 간 (inter-modality) 일치도 (κ=0.75)와 보통의 관측자간 일치도 (κ=0.47~0.59)를 보였다. 또한 실질 종괴와 병변 주변부 침윤을 유력한 악성 소견으로 간주하였을 때, 침윤성 췌장 담관 내 유두 종양 예측도는 (곡선하 면적 (AUC): 전산화 단층 촬영; 0.87, 자기 공명 영상; 0.88) 민감도 (94.3%) 의 상승과 함께 특이도의 유의한 감소 없이 (69.1%) 상당한 상승을 보였다.

결론: 췌장 담관 내 유두 종양의 악성도를 예측하는데 있어 전산화 단층 촬영과 자기공명 영상은 좋은 장비 간(inter-modality) 일치도와 함께 매우 유사한 진단성능을 보인다. 이는 췌장 담관내 유두 종양 환자에서 두 장비간 상호교환적 추적 관찰이 가능할 수 있다는 것을 의미한다.

주요어: 췌장, 담관내 유두 종양, 악성도, 전산화 단층 촬영, 자기 공명 영상, 자기공명 담도 췌관 조영술

학 번: 2013-22593